



Evolution of dosimetric treatment planning for pediatric total lymphoid irradiation (TLI): a single-institution experience

Carlos Ferrer¹, Concepción Huertas¹, Abrahams Ocanto², David García¹, Rodrigo Plaza¹, Cristina Mínguez¹, Patricia de la Monja¹, Anne Escribano², Antonio Pérez³, Moisés Sáez¹

¹Medical Physics and Radiation Protection Department, H.U. La Paz, Madrid, Spain

²Radiation Oncology Department, H.U. La Paz, Madrid, Spain

³Pediatric Hemato-Oncology Department, H.U. La Paz, Madrid, Spain

ABSTRACT

Background: Total lymphoid irradiation (TLI) is a conditioning regimen in allogeneic hematopoietic stem cell transplantation (allo-HSCT) which may reduce long-term toxicities attributed to other techniques, such as total body irradiation (TBI). At our institution, TLI treatments were first planned with the three-dimensional conformal radiation therapy (3D-CRT) technique and later with volumetric modulated arc therapy (VMAT). With the recent availability of a basic helical tomotherapy (HT), the possible dosimetric gain of the latter for TLI is studied.

Materials and methods: 22 pediatric patients were planned for VMAT and HT, prescribed to 8 Gy in 4 fractions. VMAT was planned with template based on a single cost function, using the Monaco treatment planning system (TPS). HT plans were planned using Accuray Precision TPS for a basic HT without the dynamic jaws feature or VOLO-Ultra algorithm. Plan quality was analyzed based on four quality indices, mean and maximum doses to planning target volume (PTV) and organs at risk (OARs), dose gradient and integral doses. Differences were analyzed with Wilcoxon signed-rank test.

Results: HT plans resulted in improved conformity (CI) and homogeneity indices (HI) ($p < 0.05$) but less steep dose gradient ($p = 0.181$). VMAT plans created larger areas with high doses within the PTV, while comparable doses to OARs, except mainly for the spinal marrow, for which a reduction of 37.7% in $D_{2\%}$ was obtained ($p < 0.05$). Integral dose for non-tumor tissue was 11.3% lower with the VMAT template ($p < 0.05$).

Conclusion: HT achieves better conformity and homogeneity even without its more advanced features. Nevertheless, the VMAT template achieves dosimetric results close to those of HT, both with similar clinical outcome.

Key words: total lymphoid irradiation; VMAT; tomotherapy

Rep Pract Oncol Radiother 2023;28(6):772-783

Introduction

For malignant and non-malignant oncologic disorders affecting the hematopoietic and immune system, allogeneic hematopoietic stem cell transplantation (allo-HSCT) has proven to be a rational therapeutic approach for pediatric pa-

tients [1, 2]. Conditioning regimens contribute to the stem cell engraftment and improve allo-HSCT outcome [3]. In the management of allo-HSCT, total body irradiation (TBI) has been extensively used as a conditioning regimen to induce immunosuppression for bone marrow transplantation and prevent donor marrow rejection [4-6]. TBI

Address for correspondence: Carlos Ferrer, Medical Physics and Radiation Protection Department, H.U. La Paz, Paseo de la Castellana 261, 28046, Madrid, Spain; e-mail: carlos.ferrer@salud.madrid.org

This article is available in open access under Creative Commons Attribution-Non-Commercial-No Derivatives 4.0 International (CC BY-NC-ND 4.0) license, allowing to download articles and share them with others as long as they credit the authors and the publisher, but without permission to change them in any way or use them commercially

can cause acute and late toxicities, including lethal pulmonary complications, pneumonitis, renal toxicity or veno-occlusive disease of the liver, as well as xerostomia, cardiac disease, cataracts or the development of radiation-induced secondary tumors [7, 8]. Consequently, more targeted radiation techniques have been implemented, such as total marrow irradiation (TMI), total lymphoid irradiation (TLI) and the combination of both (TMLI) [9].

The first TLI patients were treated between February 1979 and July 1981 in combination with conventional agents to prevent rejection [10]. TLI is a reduced intensity regime to induce cytopenia compared to TBI (myeloablative regimen) [11] which focus mainly on T cells to generate a state of immunosuppression, with rapid recovery of neutropenia [12], showing superior graft survival compared to another group of patients treated only with conventional immunosuppression and who did not receive TLI treatment. Even patients with drugs like alemtuzumab, muromonab (OKT3), anti-thymocyte globulin (ATG), fludarabine and thiotepa [13] showed good clinical results but with greater adverse effects compared to those described for TLI [11].

The traditional 3D conformal radiotherapy (3D-CRT) planning, which consists of two parallel opposed anterior and posterior fields: a supradiaphragmatic mantle field and an infradiaphragmatic inverted Y field [14], does not spare any organs within the field and could cause acute and late morbidities [15]. Nowadays, improved technology allows the sparing of non-lymphoid structures while delivering the prescribed dose conformed to the target. Several studies propose the use of helical tomotherapy (HT) for similar treatments such as TMI and TMLI as alternative to TBI [16]. Volumetric arc therapy (VMAT) technique with a standard linear accelerator (linac) [17] is also employed for TMI treatments. These modern techniques are applied in a limited number of centers, although they demonstrate superior dosimetric results compared with 3D-CRT, with better conformity and homogeneity indices and a demonstrated decreased dose to the thyroid, heart, esophagus and pancreas [18].

There are several studies comparing treatment planning dose distributions between 3D-CRT, VMAT, HT or proton therapy for a number of different radiotherapy treatments, including TBI [19], craniospinal irradiation (CSI) [18], TMI [20]

and others [21]. All studies observe small differences between VMAT and HT, and suggest the superior conformity and homogeneity of the dose to the target with HT treatments relative to VMAT treatments. They also report an increase in normal tissue volumes receiving low doses with HT [22]. Usually, HT produces a comparable or superior plan quality in terms of target conformity and homogeneity, and in some cases also of doses to OARs in many different pathologies [23], although longer treatment times [21].

At our institution, TLI was first planned with conformal 3D-CRT, until the planning technique was changed to VMAT with a simple template to facilitate the planning process. The VMAT template was previously presented and compared with 3DCRT planning [24], and showed much better results with VMAT compared to 3D-CRT. With the availability of a basic Tomotherapy HD treatment system at our institution, without the dynamic jaws feature or the VOLO-Ultra algorithm [20], this work aims to study the possible dosimetric gain of HT over VMAT.

Materials and methods

Patient selection and setup

Twenty-two pediatric patients were selected for this study and prescribed 8 Gy in 4 fractions (Tab. 1), twelve males and ten females, ranging from 1 to 16 years of age. Due to the different ages of the patients, the length and volume of the PTV showed considerable variations. The same CT scanner was used for VMAT and HT treatment planning. An individual Moldcare vacuum cushion (QFix, Avondale, PA) was used to scan each patient on a Philips Brilliance Big Bore 16-slice CT scanner (Philips Medical, Amsterdam, the Netherlands) with 3 mm slice thickness. The arms were kept slightly away from the body to maximize the arc length in VMAT planning and avoid di-

Table 1. Patient data characteristics.

| Patient data | | |
|----------------|----------------|--------|
| Characteristic | Mean | Range |
| Age [years] | 9.14 ± 4.29 | 1–16 |
| Height [cm] | 108.71 ± 23.32 | 60–140 |
| Gender (M/F) | 12/10 | |

Table 2. Volumetric modulated arc therapy (VMAT) template with the cost functions

| Structure | Cost function | Isoconstraint | % |
|-----------|----------------|---------------|------------|
| PTV | Target Penalty | 800 | All voxels |
| | Underdose DVH | 800 | 96 |
| | Maximum Dose | 900 | |
| Patient | Conformality | 0.20–0.50 | |
| | Maximum Dose | 900 | |

PTV — planning target volume

rect beam entrance radiation. Scans were performed from the eyes to 5 cm below the inguinal lymph nodes. The patient’s position was checked during treatment using image-guided radiotherapy (IGRT) system in both linac and Tomotherapy. Since with linac, TLI treatments require two isocenters for most patients, cone beam images were obtained for each isocenter. Each cone beam was used to position the patient at each isocenter independently. Only longitudinal table shifts were done between isocenters. With the Tomotherapy system, a scan of the entire treatment was acquired prior to each treatment fraction.

Contouring of target and OARs

The patient’s CT scans were transferred to Monaco treatment planning system (TPS) (v. 5.11.03.) (Elekta AB, Stockholm, Sweden). The PTV was created by 1 cm CTV expansion and included the lymph nodes, from the tonsil to the inguinal lymph nodes, and the spleen. Several OARs were contoured: eyeballs, eye lens, optic chiasm, external auditory canals (EACs), parotid glands, temporomandibular joint (TMJ), mandible, thyroid gland, larynx, esophagus, lungs, heart, liver, stomach, kidneys, spinal marrow, bowel, rectum, bladder, femoral heads, and gonads.

VMAT

All treatments were planned in Monaco TPS with the same template, on an Elekta Synergy linac with 6 MV nominal energy, equipped with a 160-leaf Agility multileaf collimator (MLC). Monaco TPS uses physical and biological cost functions and the XVMC Montecarlo algorithm [25]. Most VMAT plans required 2 isocenters, the first located above the manubrium and the other 25 cm away in the caudal direction. To avoid patient’s arms and shoulders irradiation, 2 partial arcs were planned for each isocenter (290° – 70°

and 135° – 210°). To optimize the overlap length and avoid the need for a third isocenter, the collimator angles were set at 5 and 340 degrees, resulting in a low gradient junction length of 25 cm, well controlled by the TPS and contributing to the plan robustness [26, 27]. That also reduces the cumulative effects of interleaf transmission and the tongue and groove effect [21]. Maximum dose rate was 600 MU/min.

The Monaco template (Tab. 2) consists of cost functions for the target and a single cost function for all voxels of the patient structure, excluding those assigned to the PTV. This cost function is named conformality, and forces the dose gradient close to the PTV. The main characteristics of this template and its comparison with 3D-CRT treatment planning were previously reported²⁴. PTV dose coverage goal was for at least 95% of the PTV volume to receive 100% of the prescribed dose (V95 ≥ 100%).

To verify patient position, kV cone-beam images were acquired prior to treatment for each isocenter. The dose optimization to the junction area wasn’t explicitly controlled, since it was observed that it is feasible to rely on the optimization algorithm with VMAT [28].

HT

Patient scans were transferred from Monaco to Accuray Precision TPS (v. 2.0.1.1.) which utilizes a convolution/superposition algorithm [29]. Plans were generated for a Tomotherapy HD with 6 MV nominal energy, binary MLC and without a flattening filter. Neither dynamic jaws nor the VOLO-Ultra algorithm were available at our center. All HT treatments were initially planned with 5 cm field width, fixed jaws, pitch value of 0.430, modulation factor of 3 and fine dose calculation grid. Due to differences in PTV volume and length values between patients, pitch and MF had to be modified for cer-

tain cases. The nominal dose rate at the isocenters was 850 cGy/min. All plans shared the same target coverage goal as the VMAT plans, $V_{95} \geq 100\%$.

Two rings were included in the HT plans to control the dose fall-off within the patient volume. The first ring, 1.5 cm wide, is contoured 0.1 cm from the PTV, followed by the second ring, 1 cm wide. To verify patient positioning, megavoltage-based CT (MVCT) images were acquired prior to the treatment.

Plan comparison

Four indices were analyzed for all plans to compare both types of treatment planning, conformity index (CI), homogeneity index (HI), conformation number (CN) and gradient index (GI). The CI was initially defined for radiosurgery treatments by Shaw et al. [30], and consists of the prescription isodose volume (V_{pi}) divided by the PTV volume (V_T). A CI value close to 1 indicates perfect conformation although a value less than 1.5 is acceptable.

$$CI = \frac{V_{pi}}{V_T} \quad (1)$$

HI in this work follows the definition suggested in ICRU 83 [31], calculated as $D_{2\%}$ minus $D_{98\%}$ divided by $D_{50\%}$ (doses received by 2%, 98% and 50% of the PTV). An HI of zero indicates that the absorbed dose distribution is almost homogeneous.

$$HI = \frac{D_{2\%} - D_{98\%}}{D_{50\%}} \quad (2)$$

CN was adopted as a tool to assess quantitatively the degree of conformality [32]. CN is calculated as the square of the PTV volume covered by the prescription isodose divided by the total PTV volume and the prescription isodose volume. A value greater than 0.6 is required, and 1 indicates the best achievable conformity.

$$CN = \frac{V_{T,pi}^2}{V_T \cdot V_{pi}} \quad (3)$$

GI was defined to differentiate plans with similar CI but different dose fall-off for stereotactic radiosurgery treatments [33] and is calculated as the volume covered by the 50% of the prescription isodose ($V_{50\%,pi}$) divided by the volume covered by the prescription isodose. A value of 3 is expected for SRS treatments, but a value around 3–6 is expected for treatments other than SRS.

$$CN = \frac{V_{T,pi}^2}{V_T \cdot V_{pi}} \quad (4)$$

For both VMAT and HT planning, the mean and maximum PTV doses at 2% of the volume ($D_{2\%}$) were registered, as well as the dose received by the 95% of the PTV volume ($D_{95\%}$). The PTV volume receiving 100% ($V_{100\%}$) and 107% ($V_{107\%}$) of the prescription dose was also noted, along with the mean MU for VMAT treatments and treatment times. Integral doses (ID) and integral doses to non-tumor tissue ID(NTT) were calculated following the description given by D'Arienzo et al. [34] For each patient, dose to 2% of the volume ($D_{2\%}$) as an indicator of the maximum dose, the mean doses to OARs and the volume receiving more than 8 Gy (V_{8Gy}) were compared. The treatment time was obtained from beam-on treatment time. IGRT time was also considered, as this time can significantly extend the overall treatment time.

Statistical analysis

Nonparametric related samples Wilcoxon signed ranks test was used to determine the possible statistically significant differences between treatment modalities for each parameter considered. The analysis was carried out with SPSS statistical software (v. 20, IBM SPSS, Armonk, NY, USA). A p-value < 0.05 was considered statistically significant.

Results

PTV and treatment parameters

As shown in Table 3, for VMAT treatments mean conformity value was 0.29 ± 0.08 , and total mean monitor units (MU) were 2647.8 ± 694.6 MU. For HT treatments, pitch and modulation factor mean values were 0.430 and 3, respectively. For most patients, beam on time and mean MU were 675.21 ± 154.08 s and 9565.48 ± 2182.8 MU.

Table 4 presents the PTV data extracted from the dose-volume histograms (DVHs) as well as the indices analyzed and the calculated integral dose. The mean PTV volume was 1714.26 ± 801.44 cc. This variability is due to the wide range in patient ages, and PTV lengths registered, 54.29 ± 9.79 cm.

PTV mean doses and $D_{2\%}$ were slightly lower with HT (1.3% and 3.9% lower, respectively) ($p < 0.05$). The PTV volume receiving more than

Table 3. Final mean values for main treatment planning parameters

| VMAT | |
|--------------------|------------------|
| Conformality | 0.29 ± 0.08 |
| MU | 2647.8 ± 694.6 |
| Treatment time [s] | 820.15 ± 150.05 |
| HT | |
| Pitch | 0.430 ± 0.02 |
| Modulation factor | 3.15 ± 0.50 |
| MU | 9565.48 ± 2182.8 |
| Treatment time [s] | 675.21 ± 154.08 |

VMAT — volumetric modulated arc therapy; HT — helical tomotherapy; MU — Monitor unit

107% of the prescribed dose (V_{107}) was much lower for HT compared with VMAT, achieving lower volumes with high doses within the PTV. Specifically, V_{107} with HT was 73.1% lower than with VMAT ($p < 0.05$). PTV coverage (V_{100}) and D_{98} with VMAT or HT were comparable.

HT treatment plans were more conformed ($CI = 1.22 \pm 0.08$) and homogeneous ($HI = 0.09 \pm 0.05$) compared to VMAT ($CI = 1.34 \pm 0.10$ and $HI = 0.13 \pm 0.04$) ($p < 0.05$). CN achieved with HT ($CN = 0.78 \pm 0.05$) was also better than with VMAT (0.71 ± 0.05) ($p < 0.05$). GI was slightly better for VMAT, but this difference wasn't statistically significant ($p = 0.181$).

ID values were 6.1% lower with VMAT, but not statistically significant ($p = 0.148$). ID(NTT) was 11.3% lower with VMAT and this difference was statically significant ($p = 0.043$). The HT plans presented shorter mean treatment times than the VMAT plans ($p = 0.001$).

OARs

The mean doses were comparable between both types of plans for most of the OARs (Tab. 5), although they were generally lower in the HT plans. Statistically significant differences with lower D_{mean} with VMAT were obtained in parotids, TMJ, humeral heads, liver and gonads (40%, 75.7%, 38.9%, 15.7% and 55.2 % lower, respectively). In contrast, statistically significant differences were obtained in the right kidney with lower D_{mean} with HT (19.5%). Lower D_{mean} also occurred for HT plans in the mandible, spinal cord, thyroid gland, larynx, esophagus, chest, heart, stomach, left kidney, vertebral body, bladder, and femoral heads, but these differences were not statistically significant. D_{mean} received in the lungs was 8.2% lower with VMAT, but this result was not statistically significant either.

$D_{2\%}$ values in Table 5 were comparable or lower for most OARs in HT plans. Among the OARs, $D_{2\%}$ values were lower with HT versus VMAT for breast, spinal marrow, right kidney, bladder, femoral heads and heart (37.7 %, 18.1%, 11.3%, 8.4%,

Table 4. Planning target volume (PTV) averaged parameters (mean ± SD), evaluation indices, integral dose, treatment time and comparison p-values

| Parameter | VMAT | HT | p-value |
|---------------------------|------------------|----------------|---------|
| Length [cm] | 54.29 ± 9.79 | | – |
| Volume [cm ³] | 1714.26 ± 801.44 | | – |
| D_{mean} [cGy] | 843.23 ± 9.58 | 831.86 ± 9.51 | 0.004 |
| $D_{2\%}$ [cGy] | 889.30 ± 18.00 | 854.10 ± 16.21 | 0.000 |
| $D_{95\%}$ [cGy] | 800.50 ± 14.26 | 801.29 ± 1.85 | 0.297 |
| $D_{98\%}$ [cGy] | 786.23 ± 11.45 | 785.05 ± 6.97 | 0.668 |
| V_{100} (%) | 95.57 ± 2.17 | 95.05 ± 0.47 | 0.170 |
| V_{107} (%) | 23.83 ± 12.13 | 6.48 ± 5.63 | 0.000 |
| CI | 1.34 ± 0.10 | 1.22 ± 0.08 | 0.001 |
| HI | 0.13 ± 0.04 | 0.09 ± 0.05 | 0.001 |
| CN | 0.71 ± 0.05 | 0.78 ± 0.05 | 0.001 |
| GI | 4.35 ± 0.73 | 4.62 ± 1.11 | 0.181 |
| ID [cGy] | 334.83 ± 55.09 | 356.56 ± 53.38 | 0.148 |
| ID(NTT) [cGy] | 282.10 ± 40.42 | 318 ± 38.49 | 0.043 |

CI — conformity index; HI — homogeneity index; CN — conformation number; GI — gradient index; ID — integral doses; ID(NTT) — integral doses to non-tumor tissue

Table 5. Dmean (cGy), D2% (cGy) and V8 (%) to organs at risk (OARs) for volumetric modulated arc therapy (VMAT) and helical tomotherapy (HT) plans

| Structure | D _{mean} [cGy] | | | D _{2%} [cGy] | | | V ₈ (%) | | |
|----------------|-------------------------|----------------|---------|-----------------------|-----------------|---------|--------------------|---------------|---------|
| | VMAT | HT | p-value | VMAT | HT | p-value | VMAT | HT | p-value |
| Eye balls | 12.72 ± 2.14 | 35.88 ± 10.87 | 0.109 | 16.70 ± 5.64 | 8.32 ± 1.43 | 0.109 | 0 | 0 | 0 |
| Eye lens | 10.88 ± 2.38 | 26.20 ± 4.09 | 0.068 | 13.50 ± 3.81 | 28.20 ± 5.82 | 0.144 | 0 | 0 | 0 |
| Optic chiasm | 15.80 ± 3.53 | 15.80 ± 3.54 | 0.109 | 19.75 ± 4.74 | 8.32 ± 2.43 | 0.109 | 0 | 0 | 0 |
| EACs | 630.03 ± 7.49 | 644.02 ± 12.73 | 0.180 | 621.95 ± 4.31 | 700.50 ± 21.92 | 0.180 | 0 | 0 | 0 |
| Parotids | 277.72 ± 30.56 | 463.17 ± 54.64 | 0.028 | 661.13 ± 95.20 | 632.20 ± 32.90 | 0.893 | 9.05 ± 1.57 | 2.58 ± 1.43 | 0.068 |
| TMJ | 122.93 ± 21.99 | 505.38 ± 85.35 | 0.008 | 356.27 ± 67.66 | 667.50 ± 93.85 | 0.028 | 0 | 0 | 0 |
| Mandible | 683.10 ± 112.06 | 674.54 ± 83.83 | 0.064 | 867.92 ± 19.24 | 827.42 ± 19.56 | 0.020 | 31.66 ± 13.62 | 25.53 ± 15.21 | 0.023 |
| Thyroid gland | 778.34 ± 33.23 | 751.07 ± 85.04 | 0.363 | 860.08 ± 40.97 | 832.29 ± 12.96 | 0.019 | 41.71 ± 12.73 | 37.95 ± 17.19 | 0.594 |
| Larynx | 753.28 ± 39.49 | 727.85 ± 68.82 | 0.221 | 857.47 ± 28.19 | 827.09 ± 23.76 | 0.011 | 31.91 ± 16.78 | 27.24 ± 16.56 | 0.347 |
| Esophagus | 810.39 ± 19.61 | 804.07 ± 15.49 | 0.272 | 877.64 ± 17.09 | 846.23 ± 16.02 | 0.013 | 77.55 ± 11.22 | 75.1 ± 12.27 | 0.272 |
| Humeral Heads | 237.54 ± 55.34 | 388.90 ± 83.26 | 0.012 | 544.16 ± 105.78 | 615.50 ± 114.79 | 0.123 | 0 | 0 | 0 |
| Breast | 362.79 ± 57.28 | 334.46 ± 62.35 | 0.500 | 777.28 ± 60.66 | 484.54 ± 58.92 | 0.144 | 1.94 ± 1.46 | 0.76 ± 0.03 | 0.068 |
| Lungs | 501.14 ± 72.30 | 545.67 ± 90.08 | 0.058 | 842.33 ± 18.43 | 827.11 ± 15.81 | 0.022 | 8.87 ± 2.85 | 10.07 ± 3.75 | 0.394 |
| Heart | 545.34 ± 81.11 | 527.14 ± 92.61 | 0.421 | 839.94 ± 28.02 | 815.89 ± 23.94 | 0.000 | 8.46 ± 1.54 | 7.71 ± 1.08 | 0.077 |
| Liver | 308.63 ± 57.41 | 366.19 ± 97.25 | 0.007 | 749.36 ± 76.17 | 756.42 ± 65.22 | 0.557 | 1.72 ± 0.40 | 1.69 ± 0.46 | 0.498 |
| Stomach | 680.98 ± 79.12 | 655.71 ± 33.17 | 0.173 | 857.90 ± 29.35 | 831.57 ± 46.26 | 0.138 | 25.13 ± 1.84 | 28.76 ± 2.65 | 0.917 |
| Right kidney | 391.14 ± 62.39 | 314.81 ± 54.22 | 0.000 | 666.83 ± 106.46 | 591.68 ± 101.00 | 0.048 | 1.27 ± 0.83 | 1.75 ± 0.85 | 0.155 |
| Left kidney | 557.77 ± 61.76 | 553.14 ± 86.79 | 0.848 | 791.76 ± 104.13 | 825.74 ± 20.24 | 0.372 | 11.85 ± 2.02 | 8.76 ± 1.43 | 0.046 |
| Brain stem | 122.30 ± 40.74 | 211.75 ± 13.91 | 0.109 | 471.53 ± 73.33 | 409.25 ± 42.15 | 0.285 | 0 | 0 | 0 |
| Spinal marrow | 540.43 ± 91.62 | 466.20 ± 77.09 | 0.061 | 731.64 ± 72.57 | 598.93 ± 105.01 | 0.005 | 2.61 ± 1.81 | 0.91 ± 0.51 | 0.173 |
| Vertebral body | 634.01 ± 69.87 | 575.10 ± 83.12 | 0.075 | 733.55 ± 20.26 | 834.22 ± 11.28 | 0.753 | 17.6 ± 1.53 | 10.52 ± 2.41 | 0.028 |
| Bowel | 414.00 ± 46.73 | 454.43 ± 66.16 | 0.128 | 837.42 ± 54.56 | 815.04 ± 67.88 | 0.018 | 9.83 ± 3.05 | 11.41 ± 2.04 | 0.570 |
| Rectum | 604.29 ± 99.50 | 618.27 ± 86.77 | 0.865 | 820.19 ± 47.53 | 824.57 ± 18.93 | 0.397 | 9.23 ± 3.26 | 13.96 ± 4.74 | 0.570 |
| Bladder | 543.19 ± 80.16 | 534.06 ± 70.59 | 0.896 | 807.26 ± 86.81 | 739.10 ± 207.48 | 0.011 | 5.69 ± 2.50 | 9.64 ± 3.73 | 0.586 |
| Femoral heads | 452.21 ± 99.06 | 446.59 ± 97.58 | 0.868 | 749.69 ± 92.74 | 699.86 ± 102.84 | 0.016 | 1.61 ± 0.31 | 2.24 ± 1.15 | 0.480 |
| Gonads | 101.24 ± 88.59 | 226.33 ± 78.52 | 0.028 | 296.80 ± 86.81 | 418.00 ± 59.30 | 0.068 | 0 | 0 | 0 |

EAC — external auditory canal; TMJ — temporomandibular joint

6.6% and 2.8% lower, respectively). In contrast, lower $D_{2\%}$ were obtained for VMAT in **TMJ**, vertebral body, humeral heads, left kidney and gonads (46.6 %, 12.1%, 11.6%, 4.1% and 29% lower, respectively). All these differences were statistically significant.

The values of the volume receiving a higher dose than prescribed, V_{8Gy} , as an indicator of dose fall-off within the OAR were similar in both VMAT and HT plans (Tab. 5), except for the mandible, left kidney and vertebral body. For these OARs, statistically significant lower values are reported for HT plans, (19.4%, 26.1% and 40.2% lower, respectively). Although not statically significant, lower V_{8Gy} values were found for VMAT plans compared with HT plans mainly in the lungs, bowel, rectum and bladder (11.9%, 13.8%, 33.9%, 40% lower respectively). The large variations between patient characteristics and contoured volumes produce the high standard deviations observed.

Discussion

This study aims to determine whether a basic Tomotherapy can improve the dosimetry of TLI treatments for patient conditioning prior to stem cell transplantation that were planned with VMAT in a conventional linac by comparing the results of both systems. Previous studies on dosimetric comparison between VMAT and HT in similar treatments, such as CSI or TMR, report the superior target conformity and homogeneity of the latter technique and comparable OAR sparing [35]. For this reason, HT has been considered as a possible dosimetric improvement over VMAT, even in its most basic version.

PTV and treatment parameters

Both VMAT and HT plans provided comparable PTV coverage, but higher doses were obtained with VMAT within the PTV, as shown by the V_{107} value obtained. Although the VMAT template includes a maximum dose cost function set to 900 cGy, the conformality cost function conforms to the prescription isodose close to the target volume and greatly increases V_{107} . Therefore, larger high-dose areas within the PTV are obtained with the VMAT template, which was previously observed by several authors [36]. Likewise, D_{mean} and $D_{2\%}$ value with VMAT resulted also higher than

the HT value. Based on the Wilcoxon signed-rank test, these differences between the VMAT and HT plans are statistically significant. The remaining dosimetric values analyzed, $D_{98\%}$, $D_{95\%}$ and V_{100} , are close for VMAT and HT, since both achieve comparable target coverage.

CI, HI and CN were improved in HT plans, which resulted in more conformed and homogeneous plans ($p < 0.05$). GI values were better with VMAT probably because the cost function in the VMAT template, conformality, affects the entire patient volume, except the PTV, whereas in HT the plan conformality is controlled by the 2 rings created, leaving the rest of the patient volume partially uncontrolled. When rings were not included in the HT plan, the GI value resulted higher than 6, implying that, if they are not considered, it is possible to have good HT plans in relation to PTV coverage and doses to the OAR, but with a dose fall-off that could be improved. This could also be somewhat resolved by adding a restriction to the total patient volume.

VMAT plans achieved lower ID(NTT) values, as larger volumes of normal tissues are exposed to low doses in HT plans [37] volumetric modulated arc therapy (VMAT. This result is consistent with other published studies [38, 39], and may be due to partial arcs with VMAT versus full arc with HT, as reported by other authors [40], although some works reflect that the integral dose delivered is mostly independent of the total number of beam angles [41]. This result is important for pediatric patients, as stated in the AAPM TG-158 report [42] which notes the increased susceptibility to second malignancies in childhood cancer patients. HT results could be improved if the dynamic jaw option were available at our institution, and substantially lower ID due to smaller dose penumbra would be delivered [43, 44].

In contrast to other studies [22], treatment time was longer with VMAT due to the need for two isocenters and double arcs, since a single arc did not meet the template objectives. Thus, the faster speed of delivery with VMAT [21] doesn't take place in this case.

In addition, the use of two isocenters could lead to setup errors, although only longitudinal table shifts are performed between both. Zhou et al. [45] studied the impact of setup errors on multi-isocenter VMAT for CSI, and demonstrated that posi-

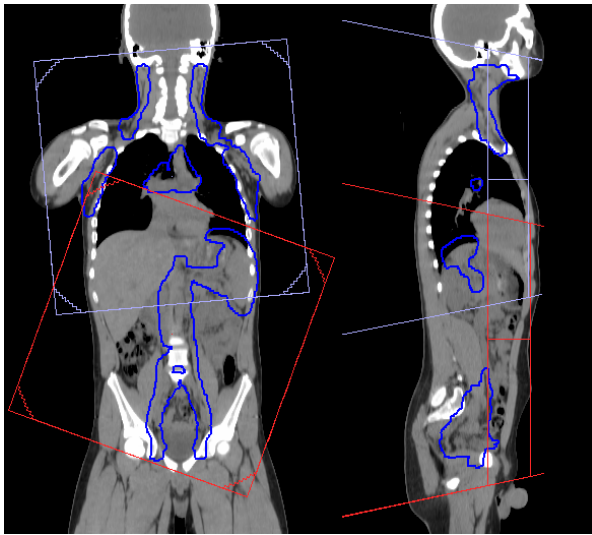


Figure 1. Collimator setting with 5° and 340° rotation used for overlap technique. Planning target volume (PTV) is outlined by blue line

tional errors within 3 mm have a little impact for VMAT CSI. Results on QA for the junction area in TLI treatments were previously described [24] and agree with other authors [28] on the feasibility

of reliance on the optimization algorithm. This issue doesn't take place with HT, as a whole scan is performed, and inter- and intrafractional errors were considered acceptable [46].

OARs

Although other works reported lower doses to OAR with HT compared to VMAT for similar treatments such as CSI [47], this wasn't the case for all OARs in this study. Some OARs show higher D_{mean} with HT than with VMAT, because in VMAT the radiation doesn't enter or exit at all through the sides of the patient, so the dose received through those areas is lower. D_{mean} to the heart was slightly lower in HT, which may reduce secondary cancers as well as cardiac complications [48]. HT results could be improved by using the dynamic jaws feature, although for large volumes and a 5-cm field size, the results in terms of OAR exposure are similar with or without this feature [43].

Figure 2 shows better $D_{50\%}$ dose distribution with HT, due to the better CI obtained compared to VMAT. HT reduced the maximum doses ($D_{2\%}$) in most OARs and improved the dose fall-off ($V_{8\%}$).

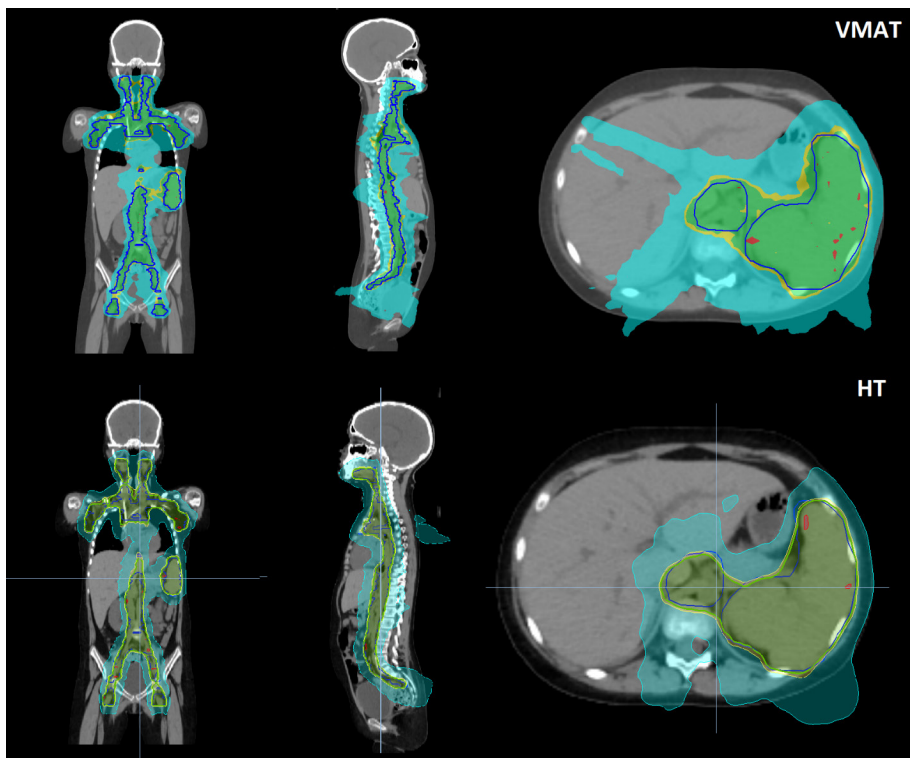


Figure 2. Isodose curves of 1 patient in sagittal, coronal and transverse sections for volumetric modulated arc therapy (VMAT) and helical tomotherapy (HT). Blue line corresponds to the planning target volume (PTV) contour. Dose fill colors red, green, yellow and cyan represent 900, 800 (prescribed dose), 860 and 400 cGy respectively

However, the differences were not significant, except mainly for the spinal marrow (Fig. 3). Results in Figure 3 showed the superior sparing for most OARs with HT, but this difference is not as great as that reported by other authors [20], which allows the conclusion that the VMAT template proposed in this work can be a good planning option if an HT is not available. Doses to the eyes, optic nerves and chiasm are slightly higher with HT due to the lack of the dynamic jaw feature.

It is worth noting that the differences between algorithms, superposition/convolution for HT and XVMC Montecarlo for Monaco, account for electron transport in different ways, and these differences are more pronounced in areas which include more bone and soft tissue boundaries,

which may cause some of the observed differences [29].

The difference in dose rate between VMAT (600 cGy/min) and HT (850 cGy/min) don't seem large enough to achieve the reported benefits in avoiding pulmonary pneumonitis [49] or renal function affection [50] when reducing the dose rate to less than 15 cGy/min in patients undergoing TBI treatments. No differences in clinical outcomes have been reported between patients undergoing allogeneic HSCT with planned TLI treatment with VMAT or HT, and good results are being obtained even in the most complex cases [51].

Finally, it should be emphasized that this planning comparison is made with respect to the planned HT treatment in our institution, which

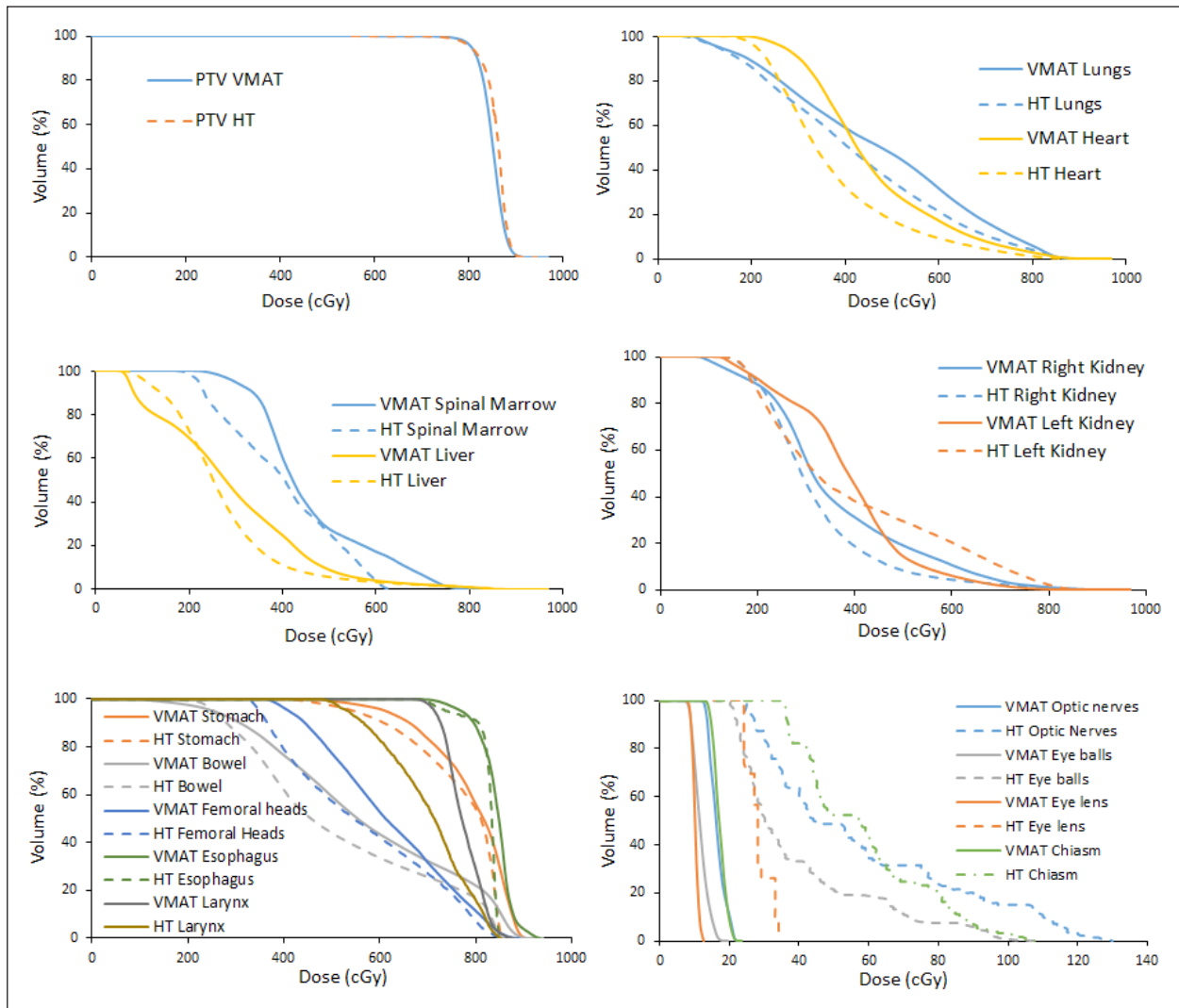


Figure 3. Volumetric modulated arc therapy (VMAT) and helical tomotherapy (HT) dose-volume histogram (DVH) comparison for planning target volume (PTV), heart, lungs, liver, bone marrow and kidneys for one patient

could probably be improved, and with it, the results achieved.

Conclusion

The results obtained reflect better dosimetric results for HT planning, besides the possibility of avoiding the use of 2 isocenters. Furthermore, HT plans showed better homogeneity and conformity, although special care should be taken when planning with HT, as the GI and, consequently, the dose fall-off, may not be optimal. The VMAT template was able to provide plan quality close to that obtained with HT with good PTV coverage and can be a good planning solution or starting point for TLI treatments in institutions where Tomotherapy is not available.

Conflict of interest

Authors declare no conflicts of interest.

Funding

None declared.

References

- Saglio F, Zecca M, Pagliara D, et al. Occurrence of long-term effects after hematopoietic stem cell transplantation in children affected by acute leukemia receiving either busulfan or total body irradiation: results of an AIEOP (Associazione Italiana Ematologia Oncologia Pediatrica) retrospective study. *Bone Marrow Transplant.* 2020; 55(10): 1918–1927, doi: [10.1038/s41409-020-0806-8](https://doi.org/10.1038/s41409-020-0806-8), indexed in Pubmed: [31996791](https://pubmed.ncbi.nlm.nih.gov/31996791/).
- Castagnoli R, Delmonte OM, Calzoni E, et al. Hematopoietic Stem Cell Transplantation in Primary Immunodeficiency Diseases: Current Status and Future Perspectives. *Front Pediatr.* 2019; 7: 295, doi: [10.3389/fped.2019.00295](https://doi.org/10.3389/fped.2019.00295), indexed in Pubmed: [31440487](https://pubmed.ncbi.nlm.nih.gov/31440487/).
- Bacigalupo A. Hematopoietic stem cell transplants after reduced intensity conditioning regimen (RI-HSCT): report of a workshop of the European group for Blood and Marrow Transplantation (EBMT). *Bone Marrow Transplant.* 2000; 25(8): 803–805, doi: [10.1038/sj.bmt.1702385](https://doi.org/10.1038/sj.bmt.1702385), indexed in Pubmed: [10808199](https://pubmed.ncbi.nlm.nih.gov/10808199/).
- Hoeben BAW, Pazos M, Seravalli E, et al. ESTRO ACROP and SIOPE recommendations for myeloablative Total Body Irradiation in children. *Radiother Oncol.* 2022; 173: 119–133, doi: [10.1016/j.radonc.2022.05.027](https://doi.org/10.1016/j.radonc.2022.05.027), indexed in Pubmed: [35661674](https://pubmed.ncbi.nlm.nih.gov/35661674/).
- Paix A, Antoni D, Waissi W, et al. Total body irradiation in allogeneic bone marrow transplantation conditioning regimens: A review. *Crit Rev Oncol Hematol.* 2018; 123: 138–148, doi: [10.1016/j.critrevonc.2018.01.011](https://doi.org/10.1016/j.critrevonc.2018.01.011), indexed in Pubmed: [29482775](https://pubmed.ncbi.nlm.nih.gov/29482775/).
- Hoeben BAW, Pazos M, Albert MH, et al. Towards homogenization of total body irradiation practices in pediatric patients across SIOPE affiliated centers. A survey by the SIOPE radiation oncology working group. *Radiother Oncol.* 2021; 155: 113–119, doi: [10.1016/j.radonc.2020.10.032](https://doi.org/10.1016/j.radonc.2020.10.032), indexed in Pubmed: [33137397](https://pubmed.ncbi.nlm.nih.gov/33137397/).
- Della Volpe A, Ferreri AJ, Annaloro C, et al. Lethal pulmonary complications significantly correlate with individually assessed mean lung dose in patients with hematologic malignancies treated with total body irradiation. *Int J Radiat Oncol Biol Phys.* 2002; 52(2): 483–488, doi: [10.1016/s0360-3016\(01\)02589-5](https://doi.org/10.1016/s0360-3016(01)02589-5), indexed in Pubmed: [11872296](https://pubmed.ncbi.nlm.nih.gov/11872296/).
- Bradley J, Reft C, Goldman S, et al. High-energy total body irradiation as preparation for bone marrow transplantation in leukemia patients: treatment technique and related complications. *Int J Radiat Oncol Biol Phys.* 1998; 40(2): 391–396, doi: [10.1016/s0360-3016\(97\)00578-6](https://doi.org/10.1016/s0360-3016(97)00578-6), indexed in Pubmed: [9457826](https://pubmed.ncbi.nlm.nih.gov/9457826/).
- Schultheiss TE, Wong J, Liu An, et al. Image-guided total marrow and total lymphatic irradiation using helical tomotherapy. *Int J Radiat Oncol Biol Phys.* 2007; 67(4): 1259–1267, doi: [10.1016/j.ijrobp.2006.10.047](https://doi.org/10.1016/j.ijrobp.2006.10.047), indexed in Pubmed: [17336225](https://pubmed.ncbi.nlm.nih.gov/17336225/).
- Slavin S. Total lymphoid irradiation. *Immunol Today.* 1987; 8(3): 88–92, doi: [10.1016/0167-5699\(87\)90852-8](https://doi.org/10.1016/0167-5699(87)90852-8), indexed in Pubmed: [25289473](https://pubmed.ncbi.nlm.nih.gov/25289473/).
- Ocanto A, Escribano A, Glaría L, et al. TLI in pediatric patients. *Clin Transl Oncol.* 2020; 22(6): 884–891, doi: [10.1007/s12094-019-02205-9](https://doi.org/10.1007/s12094-019-02205-9), indexed in Pubmed: [31542864](https://pubmed.ncbi.nlm.nih.gov/31542864/).
- Inamoto Y, Suzuki R, Kuwatsuka Y, et al. Long-term outcome after bone marrow transplantation for aplastic anemia using cyclophosphamide and total lymphoid irradiation as conditioning regimen. *Biol Blood Marrow Transplant.* 2008; 14(1): 43–49, doi: [10.1016/j.bbmt.2007.06.015](https://doi.org/10.1016/j.bbmt.2007.06.015), indexed in Pubmed: [18158960](https://pubmed.ncbi.nlm.nih.gov/18158960/).
- Phillips EH, Devereux S, Radford J, et al. Toxicity and efficacy of alemtuzumab combined with CHOP for aggressive T-cell lymphoma: a phase 1 dose-escalation trial. *Leuk Lymphoma.* 2019; 60(9): 2291–2294, doi: [10.1080/10428194.2019.1576870](https://doi.org/10.1080/10428194.2019.1576870), indexed in Pubmed: [30773077](https://pubmed.ncbi.nlm.nih.gov/30773077/).
- Heinzelmann F, Lang PJ, Ottinger H, et al. Immunosuppressive total lymphoid irradiation-based reconditioning regimens enable engraftment after graft rejection or graft failure in patients treated with allogeneic hematopoietic stem cell transplantation. *Int J Radiat Oncol Biol Phys.* 2008; 70(2): 523–528, doi: [10.1016/j.ijrobp.2007.06.037](https://doi.org/10.1016/j.ijrobp.2007.06.037), indexed in Pubmed: [17869449](https://pubmed.ncbi.nlm.nih.gov/17869449/).
- Chin C, Hunt S, Robbins R, et al. Long-term follow-up after total lymphoid irradiation in pediatric heart transplant recipients. *J Heart Lung Transplant.* 2002; 21(6): 667–673, doi: [10.1016/s1053-2498\(01\)00772-0](https://doi.org/10.1016/s1053-2498(01)00772-0), indexed in Pubmed: [12057700](https://pubmed.ncbi.nlm.nih.gov/12057700/).
- Haraldsson A, Engellau J, Lenhoff S, et al. Implementing safe and robust Total Marrow Irradiation using Helical Tomotherapy - A practical guide. *Phys Med.* 2019; 60: 162–167, doi: [10.1016/j.ejmp.2019.03.032](https://doi.org/10.1016/j.ejmp.2019.03.032), indexed in Pubmed: [31000078](https://pubmed.ncbi.nlm.nih.gov/31000078/).
- Mancosu P, Cozzi L, Muren LP. Total marrow irradiation for hematopoietic malignancies using volumetric modulated arc therapy: A review of treatment planning studies. *Phys Imaging Radiat Oncol.* 2019; 11: 47–53, doi: [10.1016/j.phro.2019.08.001](https://doi.org/10.1016/j.phro.2019.08.001), indexed in Pubmed: [33458277](https://pubmed.ncbi.nlm.nih.gov/33458277/).

18. Seravalli E, Bosman M, Lassen-Ramshad Y, et al. Dosimetric comparison of five different techniques for craniospinal irradiation across 15 European centers: analysis on behalf of the SIOP-E-BTG (radiotherapy working group). *Acta Oncol.* 2018; 57(9): 1240–1249, doi: [10.1080/0284186X.2018.1465588](https://doi.org/10.1080/0284186X.2018.1465588), indexed in Pubmed: [29698060](https://pubmed.ncbi.nlm.nih.gov/29698060/).
19. Loginova AA, Kobyzeva DA, Tovmasyan DA, et al. Comparison of total body irradiation using TomoTherapy and volume-modulated rotational radiation therapy Elekta. A single center experience on pediatric patients. *Pediatr Hematol/Oncol Immunopathol.* 2019; 18(4): 49–57, doi: [10.24287/1726-1708-2019-18-4-49-57](https://doi.org/10.24287/1726-1708-2019-18-4-49-57).
20. Nalichowski A, Eagle DG, Burmeister J. Dosimetric evaluation of total marrow irradiation using 2 different planning systems. *Med Dosim.* 2016; 41(3): 230–235, doi: [10.1016/j.meddos.2016.06.001](https://doi.org/10.1016/j.meddos.2016.06.001), indexed in Pubmed: [27372384](https://pubmed.ncbi.nlm.nih.gov/27372384/).
21. Rao M, Yang W, Chen F, et al. Comparison of Elekta VMAT with helical tomotherapy and fixed field IMRT: plan quality, delivery efficiency and accuracy. *Med Phys.* 2010; 37(3): 1350–1359, doi: [10.1118/1.3326965](https://doi.org/10.1118/1.3326965), indexed in Pubmed: [20384272](https://pubmed.ncbi.nlm.nih.gov/20384272/).
22. Hacıislamoglu E, Colak F, Canyilmaz E, et al. Dosimetric comparison of left-sided whole-breast irradiation with 3DCRT, forward-planned IMRT, inverse-planned IMRT, helical tomotherapy, and volumetric arc therapy. *Phys Med.* 2015; 31(4): 360–367, doi: [10.1016/j.ejmp.2015.02.005](https://doi.org/10.1016/j.ejmp.2015.02.005), indexed in Pubmed: [25733372](https://pubmed.ncbi.nlm.nih.gov/25733372/).
23. Zhang Y, Wang H, Huang X, et al. Dosimetric comparison of TomoDirect, helical tomotherapy, VMAT, and ff-IMRT for upper thoracic esophageal carcinoma. *Med Dosim.* 2019; 44(2): 167–172, doi: [10.1016/j.meddos.2018.05.001](https://doi.org/10.1016/j.meddos.2018.05.001), indexed in Pubmed: [29950277](https://pubmed.ncbi.nlm.nih.gov/29950277/).
24. Ferrer C, Huertas C, Plaza R, et al. Simple template-based optimization for pediatric total lymphoid irradiation (TLI) radiotherapy treatments. *Med Dosim.* 2021; 46(2): 201–207, doi: [10.1016/j.meddos.2020.11.003](https://doi.org/10.1016/j.meddos.2020.11.003), indexed in Pubmed: [33309515](https://pubmed.ncbi.nlm.nih.gov/33309515/).
25. Clements M, Schupp N, Tattersall M, et al. Monaco treatment planning system tools and optimization processes. *Med Dosim.* 2018; 43(2): 106–117, doi: [10.1016/j.meddos.2018.02.005](https://doi.org/10.1016/j.meddos.2018.02.005), indexed in Pubmed: [29573922](https://pubmed.ncbi.nlm.nih.gov/29573922/).
26. Li Q, Gu W, Mu J, et al. Collimator rotation in volumetric modulated arc therapy for craniospinal irradiation and the dose distribution in the beam junction region. *Radiat Oncol.* 2015; 10: 235, doi: [10.1186/s13014-015-0544-z](https://doi.org/10.1186/s13014-015-0544-z), indexed in Pubmed: [26584626](https://pubmed.ncbi.nlm.nih.gov/26584626/).
27. Wang K, Meng H, Chen J, et al. Plan quality and robustness in field junction region for craniospinal irradiation with VMAT. *Phys Med.* 2018; 48: 21–26, doi: [10.1016/j.ejmp.2018.03.007](https://doi.org/10.1016/j.ejmp.2018.03.007), indexed in Pubmed: [29728225](https://pubmed.ncbi.nlm.nih.gov/29728225/).
28. Lee YK, Brooks CJ, Bedford JL, et al. Development and evaluation of multiple isocentric volumetric modulated arc therapy technique for craniospinal axis radiotherapy planning. *Int J Radiat Oncol Biol Phys.* 2012; 82(2): 1006–1012, doi: [10.1016/j.ijrobp.2010.12.033](https://doi.org/10.1016/j.ijrobp.2010.12.033), indexed in Pubmed: [21345612](https://pubmed.ncbi.nlm.nih.gov/21345612/).
29. Sterpin E, Salvat F, Olivera G, et al. Monte Carlo evaluation of the convolution/superposition algorithm of Hi-Art tomotherapy in heterogeneous phantoms and clinical cases. *Med Phys.* 2009; 36(5): 1566–1575, doi: [10.1118/1.3112364](https://doi.org/10.1118/1.3112364), indexed in Pubmed: [19544772](https://pubmed.ncbi.nlm.nih.gov/19544772/).
30. Shaw E, Kline R, Gillin M, et al. Radiation Therapy Oncology Group: radiosurgery quality assurance guidelines. *Int J Radiat Oncol Biol Phys.* 1993; 27(5): 1231–1239, doi: [10.1016/0360-3016\(93\)90548-a](https://doi.org/10.1016/0360-3016(93)90548-a), indexed in Pubmed: [8262852](https://pubmed.ncbi.nlm.nih.gov/8262852/).
31. ICRU. Prescribing, Recording, and Reporting Photon-Beam Intensity-Modulated Radiation Therapy (IMRT). *J ICRU.* 2010; 10(1): 1–3, doi: [10.1093/jicru_ndq002](https://doi.org/10.1093/jicru_ndq002).
32. van't Riet A, Mak AC, Moerland MA, et al. A conformation number to quantify the degree of conformality in brachytherapy and external beam irradiation: application to the prostate. *Int J Radiat Oncol Biol Phys.* 1997; 37(3): 731–736, doi: [10.1016/s0360-3016\(96\)00601-3](https://doi.org/10.1016/s0360-3016(96)00601-3), indexed in Pubmed: [9112473](https://pubmed.ncbi.nlm.nih.gov/9112473/).
33. Paddick I, Lippitz B. A simple dose gradient measurement tool to complement the conformity index. *J Neurosurg.* 2006; 105 Suppl: 194–201, doi: [10.3171/sup.2006.105.7.194](https://doi.org/10.3171/sup.2006.105.7.194), indexed in Pubmed: [18503356](https://pubmed.ncbi.nlm.nih.gov/18503356/).
34. D'Arienzo M, Masciullo SG, de Sanctis V, et al. Integral dose and radiation-induced secondary malignancies: comparison between stereotactic body radiation therapy and three-dimensional conformal radiotherapy. *Int J Environ Res Public Health.* 2012; 9(11): 4223–4240, doi: [10.3390/ijerph9114223](https://doi.org/10.3390/ijerph9114223), indexed in Pubmed: [23202843](https://pubmed.ncbi.nlm.nih.gov/23202843/).
35. Myers PA, Mavroidis P, Papanikolaou N, et al. Comparing conformal, arc radiotherapy and helical tomotherapy in craniospinal irradiation planning. *J Appl Clin Med Phys.* 2014; 15(5): 4724, doi: [10.1120/jacmp.v15i5.4724](https://doi.org/10.1120/jacmp.v15i5.4724), indexed in Pubmed: [25207562](https://pubmed.ncbi.nlm.nih.gov/25207562/).
36. Lu S, Fan H, Hu X, et al. Dosimetric Comparison of Helical Tomotherapy, Volume-Modulated Arc Therapy, and Fixed-Field Intensity-Modulated Radiation Therapy in Locally Advanced Nasopharyngeal Carcinoma. *Front Oncol.* 2021; 11: 764946, doi: [10.3389/fonc.2021.764946](https://doi.org/10.3389/fonc.2021.764946), indexed in Pubmed: [34804969](https://pubmed.ncbi.nlm.nih.gov/34804969/).
37. Davidson MTM, Blake SJ, Batchelar DL, et al. Assessing the role of volumetric modulated arc therapy (VMAT) relative to IMRT and helical tomotherapy in the management of localized, locally advanced, and post-operative prostate cancer. *Int J Radiat Oncol Biol Phys.* 2011; 80(5): 1550–1558, doi: [10.1016/j.ijrobp.2010.10.024](https://doi.org/10.1016/j.ijrobp.2010.10.024), indexed in Pubmed: [21543164](https://pubmed.ncbi.nlm.nih.gov/21543164/).
38. Goswami B, Jain R, Yadav S, et al. Dosimetric comparison of integral dose for different techniques of craniospinal irradiation. *J Radiother Pract.* 2020; 20(3): 345–350, doi: [10.1017/s1460396920000424](https://doi.org/10.1017/s1460396920000424).
39. Servagi Vernat S, Ali D, Puyraveau M, et al. Is IMAT the ultimate evolution of conformal radiotherapy? Dosimetric comparison of helical tomotherapy and volumetric modulated arc therapy for oropharyngeal cancer in a planning study. *Phys Med.* 2014; 30(3): 280–285, doi: [10.1016/j.ejmp.2013.07.128](https://doi.org/10.1016/j.ejmp.2013.07.128), indexed in Pubmed: [23948367](https://pubmed.ncbi.nlm.nih.gov/23948367/).
40. Sarkar B, Munshi A, Ganesh T, et al. Dosimetric comparison of short and full arc in spinal PTV in volumetric-modulated arc therapy-based craniospinal irradiation. *Med Dosim.* 2020; 45(1): 1–6, doi: [10.1016/j.meddos.2019.03.003](https://doi.org/10.1016/j.meddos.2019.03.003), indexed in Pubmed: [30995966](https://pubmed.ncbi.nlm.nih.gov/30995966/).
41. D'Souza WD, Rosen II. Nontumor integral dose variation in conventional radiotherapy treatment planning. *Med Phys.* 2003; 30(8): 2065–2071, doi: [10.1118/1.1591991](https://doi.org/10.1118/1.1591991), indexed in Pubmed: [12945972](https://pubmed.ncbi.nlm.nih.gov/12945972/).
42. Kry SF, Bednarz B, Howell RM, et al. AAPM TG 158: Measurement and calculation of doses outside the treated volume from external-beam radiation therapy. *Med Phys.* 2017; 44(10): e391–e429, doi: [10.1002/mp.12462](https://doi.org/10.1002/mp.12462), indexed in Pubmed: [28688159](https://pubmed.ncbi.nlm.nih.gov/28688159/).

43. Krause S, Beck S, Schubert K, et al. Accelerated large volume irradiation with dynamic Jaw/Dynamic Couch Helical Tomotherapy. *Radiat Oncol.* 2012; 7: 191, doi: [10.1186/1748-717X-7-191](https://doi.org/10.1186/1748-717X-7-191), indexed in Pubmed: [23146914](https://pubmed.ncbi.nlm.nih.gov/23146914/).
44. Sterzing F, Uhl M, Hauswald H, et al. Dynamic jaws and dynamic couch in helical tomotherapy. *Int J Radiat Oncol Biol Phys.* 2010; 76(4): 1266–1273, doi: [10.1016/j.ijrobp.2009.07.1686](https://doi.org/10.1016/j.ijrobp.2009.07.1686), indexed in Pubmed: [19910128](https://pubmed.ncbi.nlm.nih.gov/19910128/).
45. Zhou Y, Ai Y, Han Ce, et al. Impact of setup errors on multi-isocenter volumetric modulated arc therapy for craniospinal irradiation. *J Appl Clin Med Phys.* 2020; 21(11): 115–123, doi: [10.1002/acm2.13044](https://doi.org/10.1002/acm2.13044), indexed in Pubmed: [33070426](https://pubmed.ncbi.nlm.nih.gov/33070426/).
46. Lee J, Kim E, Kim N, et al. Practical aspects of the application of helical tomotherapy for craniospinal irradiation. *Sci Rep.* 2021; 11(1): 6120, doi: [10.1038/s41598-021-85574-y](https://doi.org/10.1038/s41598-021-85574-y), indexed in Pubmed: [33731843](https://pubmed.ncbi.nlm.nih.gov/33731843/).
47. Sun Y, Liu G, Chen W, et al. Dosimetric comparisons of craniospinal axis irradiation using helical tomotherapy, volume-modulated arc therapy and intensity-modulated radiotherapy for medulloblastoma. *Transl Cancer Res.* 2019; 8(1): 191–202, doi: [10.21037/tcr.2019.01.30](https://doi.org/10.21037/tcr.2019.01.30), indexed in Pubmed: [35116748](https://pubmed.ncbi.nlm.nih.gov/35116748/).
48. Maraldo MV, Brodin NP, Aznar MC, et al. Estimated risk of cardiovascular disease and secondary cancers with modern highly conformal radiotherapy for early-stage mediastinal Hodgkin lymphoma. *Ann Oncol.* 2013; 24(8): 2113–2118, doi: [10.1093/annonc/mdt156](https://doi.org/10.1093/annonc/mdt156), indexed in Pubmed: [23619032](https://pubmed.ncbi.nlm.nih.gov/23619032/).
49. Gao RW, Weisdorf DJ, DeFor TE, et al. Influence of Total Body Irradiation Dose Rate on Idiopathic Pneumonia Syndrome in Acute Leukemia Patients Undergoing Allogeneic Hematopoietic Cell Transplantation. *Int J Radiat Oncol Biol Phys.* 2019; 103(1): 180–189, doi: [10.1016/j.ijrobp.2018.09.002](https://doi.org/10.1016/j.ijrobp.2018.09.002), indexed in Pubmed: [30205123](https://pubmed.ncbi.nlm.nih.gov/30205123/).
50. Cheng JC, Schultheiss TE, Wong JYC. Impact of drug therapy, radiation dose, and dose rate on renal toxicity following bone marrow transplantation. *Int J Radiat Oncol Biol Phys.* 2008; 71(5): 1436–1443, doi: [10.1016/j.ijrobp.2007.12.009](https://doi.org/10.1016/j.ijrobp.2007.12.009), indexed in Pubmed: [18355974](https://pubmed.ncbi.nlm.nih.gov/18355974/).
51. Gasior M, Ferreras C, de Paz R, et al. The role of early natural killer cell adoptive infusion before engraftment in protecting against human herpesvirus-6B encephalitis after naïve T-cell-depleted allogeneic stem cell transplantation. *Transfusion.* 2021; 61(5): 1505–1517, doi: [10.1111/trf.16354](https://doi.org/10.1111/trf.16354), indexed in Pubmed: [33713461](https://pubmed.ncbi.nlm.nih.gov/33713461/).